

## WELDING CURRENT AND SHIELDING GAS FLOW RATE EFFECT TO THE INTERMETALLIC LAYER FORMATION OF TUNGSTEN INERT GAS (TIG) ON DISSIMILAR METALS WELD JOINTS BETWEEN GALVANIZED STEEL AND ALUMINIUM AA 5052 BY USING Al-Si 4043 FILLER

Gilang Sigit Saputro<sup>1</sup>, Triyono<sup>1</sup>, Nurul Muhayat<sup>1</sup>

<sup>1</sup>Teknik Mesin – Universitas Sebelas Maret

---

### **Keywords :**

*Tungsten Inert Gas welding  
dissimilar metal  
welding current  
shielding gas flowrate  
intermetallic  
hardness*

---

### **Abstract :**

Tungsten Inert Gas welding of galvanized steel-aluminium useful for weight reduction, improve perform and reduce cost production. The effect of welding parameters, welding current and shielding gas flow rate on the intermetallic formation and hardness of dissimilar metals weld joint between galvanized steel and aluminium by using AA 5052 filler was determined. In this research, welding speed was consistent kept. The welding parameters were obtained by using welding currents of 70, 80 and 90 A, shielding gas flow rate of 10, 12 and 14 litre/min. The intermetallic layer thickness increased by welding currents of 70 A to 80 A, but then it dropped on 90 A. The higher of a shielding gas flow rate, the lower the thickness of the intermetallic layer. The higher of a welding current, the lower the hardness of weld. The higher of a shielding gas flow rate, the greater the hardness of weld. As a result, the maximum hardness by current variation of 70 A and a shielding gas flow rate of 14 Litre/min was 100.9 HVN.

---

## 1. INTRODUCTION

Industrial development is rapidly growth, especially in automotive industry. Welding is widely used for the metal joining process, because it has some advantages such as strong joining, provident, cheap, and easy to apply. Many methods are used in metal welding processes. Tungsten Inert Gas (TIG) welding was selected in this study. The direct aluminum and galvanized steel welding is difficult to operate. It can be caused by a melting point big difference, thermal conductivity, incompatibility, and compound brittle intermetallic during the welding process [1].

Many studies are conducted to address these issues, such as aluminum alloys to low carbon steel with a filler metal of GTAW welding [2]. Fe-rich layer is separated from the surface during welding. Intermetallic layer has 15  $\mu\text{m}$  of thickness. The joining tensile strength was increased from 111 MPa to 150 MPa after a heat treatment. The aluminum to other galvanized steel joining experiments were using laser welding and GTAW welding [3]. Intermetallic layers, Fe-Al which fragile were easily formed under arc thus worsening the joining mechanical properties.

In this study was using TIG welding with protection argon gas and additional Al-Si 4043 as filler metal. It became necessary to find the most optimum variable in TIG welding process of galvanized steel to aluminum. Therefore, it could be reducing vehicle

weight, improving engine performance, and decreasing cost production [4].

## 2. BASIC THEORY

TIG welding is electric welding variety which are using tungsten materials as an unconsumed electrode. It serves only to conduct electricity from the power source to the essential metal. Therefore, it produces an electric arc flame which has a high thermal energy. Certain additives as filler rod was disbursed by the weld region filling arc flame. Noble gases such as argon, helium, and CO<sub>2</sub> are used as a protective gas to prevent oxidation from outside air to the liquid metal which being welded.

TIG welding is suitable for thin plate welding because it has a limited heat input. The filler metal feeding rate does not depend on the welding current. TIG welding process is very clean which can be used for the reactive metals such as titanium, zirconium, aluminum, and magnesium. Electrical currents which are too high can cause tungsten electrode melting and generate a welding brittle inclusions. The welding process uses a tungsten electrode which is not an added ingredient. Electric arc that occurs between the end of the tungsten electrode and the base material is a welding heat source. Figure 2.1 shows the TIG welding process when fusing and connecting the metal by heating it through an arc which formed from a tungsten electrode that is not consumed by the primary metal.

Its torch grip is connected to the protector gas tube as in Figure 2.1 (a). It is usually contacted to copper tube cooling water, called a contact tube as shown in Figure 2.1 (b), which is attached to the terminal welding cable. The welding electric current is flowing from the power source to the electrode and it is cooled to prevent excessive heat. Workpiece is associated to the other terminal on the power source through a different cable 2. Shielding gas enters through the torch body. It is aimed by the nozzle toward the weld pool to protect the entry air from outside environment. The GTAW welding air protection is better than GMAW from its inert gas which directly targeted to the weld pool. For this reason, GTAW welding is also referred to TIG welding.

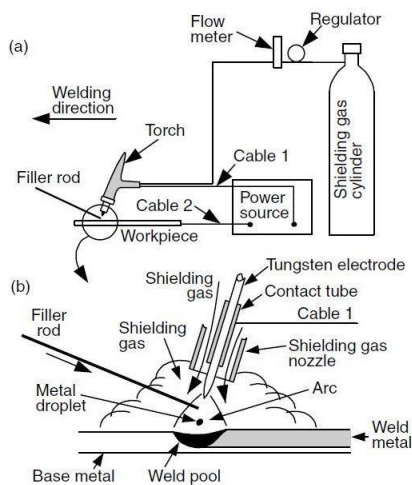


Figure. 2.1 Tungsten Inert Gas Welding, (a) whole process; (b) welding area [5].

### 3. RESEARCH METHODOLOGY

#### a. Equipment dan Materials

TIG welding machine in Figure 3.1 (a) which was used, it has 5-200 A of output current and 85% of efficiency. JIG was practiced as in Figure 3.1 (b) with such designed which is able to clamp the workpiece perfectly. Therefore, the connection density can be maintained.



i. (b)

Figure 3.1 (a) TIG Welding Machine dan (b) JIG Plate Clamp

The materials which operated as the parent metal was 200 x 80 x 3 mm of aluminum plate AA 5052 and 200 x 80 x 1.2 mm of galvanized steel, while Al-Si 4043 wire shaped of filler metal with 1.6 mm of diameter as shown in Figure 3.2 was also performed. Pure tungsten with 2.6 mm of diameter was employ which not consumed during the welding process.

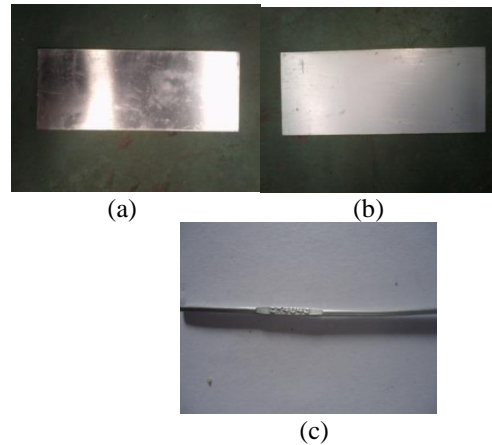


Figure 3.2 Aluminium AA 5052 as Main Metal (a), Galvanised Metal (b), dan (c) Al-Si 4043 filler.

Chemistry composition for each material is shown on Table 3.1 and Table 3.2.

Table 3.1 Chemistry composition base metal

| Type material   | % C   | % Mg    | % Cr | % Al | % Si  | % Cu | % Fe | % Zn |
|-----------------|-------|---------|------|------|-------|------|------|------|
| Baja Galvanis   | 0.050 | 3.0     | -    | 0.6  | 0,019 | -    | Bal  | -    |
| Aluminium A5052 | -     | 2.2-2.8 | 0.15 | 95.7 | 0.25  | 0.10 | 0.40 | 0.10 |

Table 3.2 Chemistry composition filler metal Al-Si 4043 [6]

| Weight%    | Al  | Si      | Fe       | Cu       | Ti       | Zn       | Mn       | Mg       | Others        |
|------------|-----|---------|----------|----------|----------|----------|----------|----------|---------------|
| Alloy 4043 | Bal | 4.5-6.0 | 0.80 max | 0.30 max | 0.20 max | 0.10 max | 0.05 max | 0.05 max | 0.05 max each |

#### b. Research Methodology Scheme

Figure 3.3 shows a research method flowchart. The independent variables that used in this study was 70 A, 80 A, 90 A of electric current and 10 L/ min, 12 L/ min, 14 L/ min of shielding gas flow rate. The dependent variable was the intermetallic layer formation and the hardness number from the TIG welding process on galvanized steel and AA 5052 of aluminum. Controlled variable was welding speed.

Determining the research scope which is preferred therefore determined boundary problem as follows:

1. A constant welding speed of 60 mm/ min.
2. Cleaning the surface of the plate is uniformly performed using alcohol.

3. Cooling welds performed in air at room temperature.

Welding process was performed by an experienced welder and has been certified by a recognized training weld institution that can ensure a uniform filet form on the outcome of the welds so it will not affect the test results in this study.

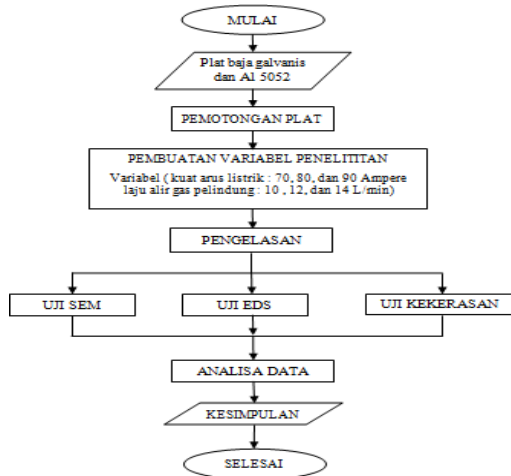


Figure 3.3. Research method flowchart

AWS D1.1 / D1.1M: 2006 was as a standard geometry for plate preparation as shown in Figure 3.4. A5052 aluminum alloy plate and galvanized steel 200 x 80 x 1.2 mm of dimensions and 25 mm of length of overlap welding connection.

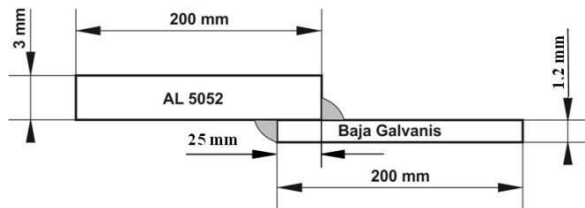


Figure 3.4 Lap joint plate configuration based on AWS D1.1/D1.1M:2006

### c. Testing

Layer formation testing was using a scanning electron microscope (SEM) and energy dispersive spectrometry (EDS), while hardness was using Vikers testing machine. SEM and EDS preparation, a welding specimen which has been connected was cut in the middle and then filed until flat. Specimens that have been refined and then polished using autosol to remove residual sanding scratches. Then, the specimens were etched with modified reagent poulton in aluminum with 6 grams  $\text{CrO}_3$  of mixture composition, 15 ml of  $\text{HCl}$ ,  $\text{HNO}_3$ , and 1.25 ml of  $\text{HF}$  which mixture by 21.25 ml of distilled water. Etsa fluid for low carbon steel galvanized using a composition mixture 1 ml of  $\text{HNO}_3$  which blended in 10 ml of distilled water. SEM

and EDS testing areas scheme is shown in Figure 3.5. Vikcers testing was conducted to determine the hardnessdistribution in aluminum base metal, heat affected zone (HAZ), and the aluminum weld using 200 gf for 10 s of loading. Vickers hardness test scheme is shown in Figure 3.6 :

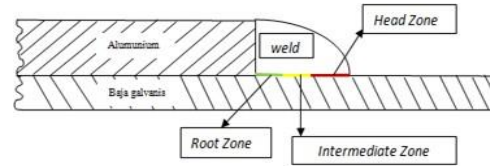


Figure 3.5. SEM dan EDS testing area [7]

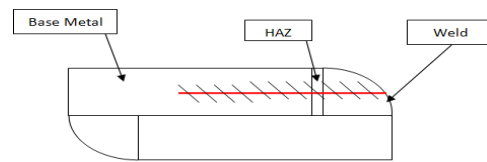


Figure 3.6. Vickers hardness testing scheme [8]

## 4. DATA ANALYSIS

### a. Intermetallic layer on Head Zone

There are 3 weld sections were tested by SEM such as, head zone, intermediate zone, and root zone. Head zone is free layer reaction part which was indicating the liquid weld on galvanized parts. At the galvanized coating head zone of steel has been destroyed and several dendrites begin to grow from the interface and there was a micro-pore shrinkage in the inter dendrites. At the intermetallic, there are 4 important atomic constituents are Fe, Al, Si, and Zn. On EDS testing was taken from 7 spectrums vertically from the welds, intermetallic layer to galvanized. For all variations, the number of atomic Fe was increased while Al was declined, while the Si atoms and Zn values were uncertain.

Figure 4.1 shows the test results on the SEM head zone for all variations. Intermetallic layer thickness will be increased from 70 A to 80 A of current and will decrease to 90 A. Si content was determining the thickness or thinness of intermetallic layer. The greater content of Si atoms will make the grain size becomes small and prevents diffusion of Fe atoms from the base metal galvanized steel, thereby reducing the thickness of the intermetallic layer and increase its tensile strength [9].

Figure 4.2 displays EDS testing result in all variations. At 70 A of current, 0.6% of Si, and then declined to 0.2%.of Si content was less cause intermetallic layer that forms were becoming increasingly bold. Intermetallic layer on 90 A of current becomes thinner. It could be caused by the

increasing 3.2% of Si content. On 12 liters/ minute of protected gas flow rate, 0.3, 0.1, and 3.5% of Si content and 14 liter/ min of gas flow hedge rate: 1.1, 0.4 and 0.9%.

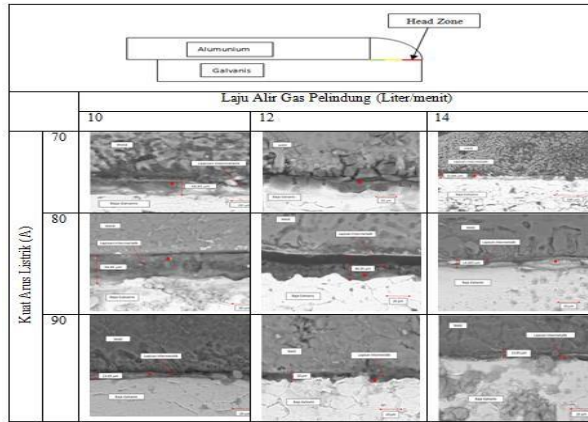


Figure 4.1. Head zone testing result

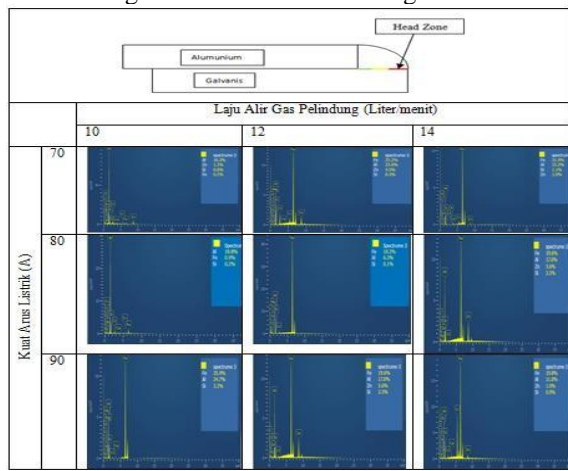


Figure 4.2. EDS testing result on head zone

Intermediate zone is part of the reaction layer with a thickness of at most. Reaction layer was formed by columnar crystals variable composition of Al and Fe. Intermetallic compounds configuration was consisting of two phases, namely  $FeAl_3$  at the aluminum and galvanized  $Fe_2Al_5$  in the nearby area [10]. Figure 4.3 shows SEM testing result at the intermediate zone for all variations. At 80 A of current by an additional thickness of the intermetallic layer thickness then decreased in 90 A of current. In 80 A of current heat input becomes larger therefore the cooling rate widened more slowly, causing the formation of  $FeAl_3$  be increased and the size becomes larger [10]. The increasing current will stimulate the thickness of the reaction layer in which the thickness of the layer decreases discontinuous reaction [11]. At 80 A of current was the peak of reaction layer. Therefore, 90 A of current reaction layer thickness will be decreased.

Figure 4.4 portrays EDS testing result at the intermediate zone for all variations. The content of 70

A of current at 1.0%, was down to 0.3% on 80 A of current and 90 A rise of current to 2.1% of the gas flow. The content 70 A of current: 0.3%, was down to 0.2% on 80 A and 90 A of current with 3.4% of Si content. Si content which was decreased at 80 A of current and an increased in 90 A of current proves that the increasing thickness of the intermetallic layer on 80 A of current and decreased thickness of the intermetallic layer on 90 A of current.

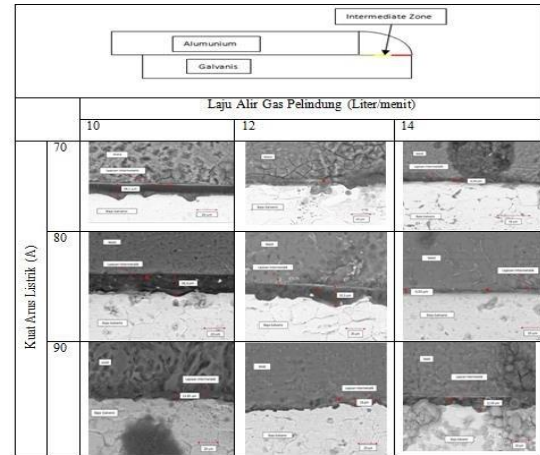


Figure 4.3 SEM testing results on Intermediate Zone

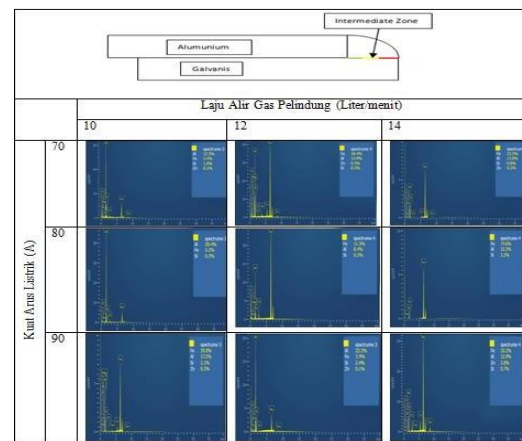


Figure 4.4 EDS testing result on Intermediate Zone

Root zone is the most complex which located between the steel and light strip where most contain zinc. From Figure 4.5 comparison, it can be seen that the greater the gas flow rate hedge for the same current, the thickness of the intermetallic layer will also be dwindling. According to the hypothesis, this is due to the same current, the greater the gas hedge rate the more gas that protects the weld from that will improve cooling rate and refine the grain size so the intermetallic layer was formed to be thinner. A deviation was occurred from the thickness of the intermetallic layer on 10 liters/ min of gas flow rate

decreased in the 12 liters/ min of gas flow rate and increased thickness in 14 liters/ minute of gas flow rate. Figure 4.6 EDS testing result on 90 A of current shows aberration reasons that Si content in the intermetallic layer. Si content in 10 liter/ min of gas flow rate hedging at 0.2% increased to 1.4% in 12 liter/ minute of gas flow rate hedging. The increasing of Si content caused the intermetallic layer becomes thinner. Si content decreased to 0.5% for 14 liter/ minute of gas flow rate hedging, so the intermetallic layer the thickness increased.

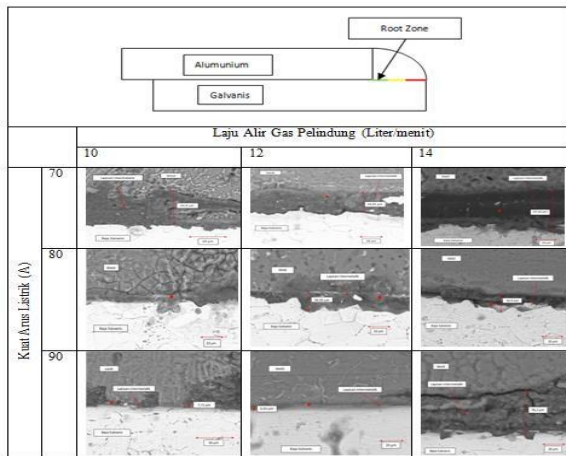


Figure 4.5 SEM testing result on root zone

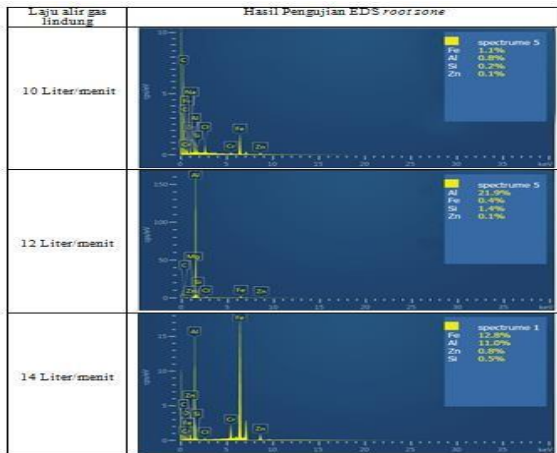


Figure 4.6. EDS testing result on root zone at 90 A of current

**b. Vickers Hardness Testing Results**

The electrical current addition is always directly proportional to the main voltage. This is in accordance with the laws of joules, increasing the electric current will also increase heat input and will cause the cooling rate (cooling rate) becomes slow. The greater the heat input will increase the size and spacing between the dendrite, which will lower the hardness [12]. It can be seen from the research results to increase the current with the same gas flow rate as shown in Figure 4.7.,

Figure 4.8., and Figure 4.9. For 10 liters/ minute of gas flow rate, the hardness average value at the weld decreased from 78.32 HV, 79.2 HV, and 72.58 HV. For 12 liters/ minute of gas flow rate, 92.02 HV, 82.5HV, and 80.54 HV, for a gas flow rate of 14 liters/ min of gas flow rate, 94.6 HV, HV 87.32, 83.8 HV were obtained. Protected gas at 10 liters/ minute of irregularities flow rate which the average weld hardness increased from 78.32 HV to 79.2 HV, due to the its content the 10 liters/ min of gas flow rate at 80 A of current was higher than 10 liters/ min of gas flow rate hedging at 70 A of current, the larger the content of Silicon, the grain size and the distance between the grains become smaller [9]. Therefore, the damage was also increased. The content of silicon in the weld test was known from EDS as shown in Figure 4.10 and Figure 4.11.

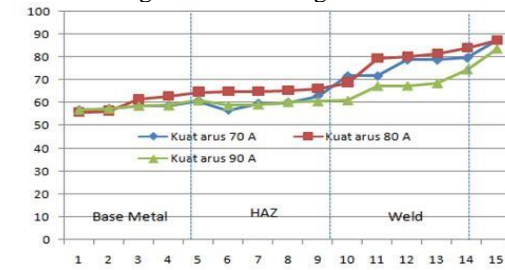


Figure 4.7 Vickers testing graph on 10 L/min

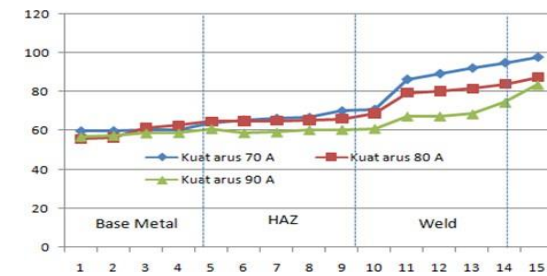


Figure 4.8 Vickers testing graph on 12 L/min

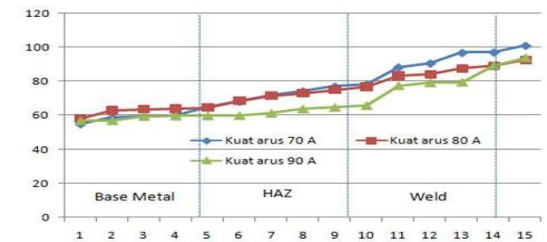


Figure 4.9 Vickers testing graph on 14 L/min

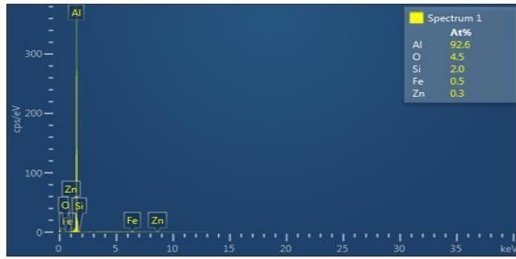


Figure 4.10 EDS testing result on 70 A, 10 L/min

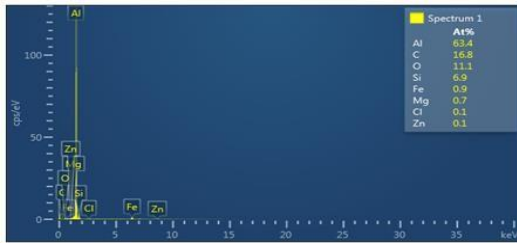


Figure 4.11 EDS testing result on 80 A, 10 L/min

Figure 4.7, Figure 4.8, and Figure 4.9 show an the increasing trend of ranging damage from aluminum base metal, aluminum heat affected zone, and welding. The highest hardness value was located in welding area due to hard of brittle intermetallic phase formation in the welding area [13]. Hard of brittle intermetallic phase as FeAl3 and Fe2Al5 will also increase hardness and lower tensile strength

The shielding gas flow rate is a parameter that indicates the number of protected gas flowing in units of liters in one minute during the welding process. The greater the shielding gas, the greater the gas to protect the weld from adverse atmospheric air. From Figure 4.12, Figure 4.13, and Figure 4.14, it can be seen that the shielding gas flow rate affect the hardness value of welding area. The greater the gas flow rate will increase hardness values as shown in Figure 4.12 average hardness weld on 70 A of current: 78.32 HV, 92.02 HV, and 94.6 HV. Figure 4.13 shows the welding average hardness on 80 A of current: 79.2 HV, 82.5 HV, and 87.32 HV. Average weld damage at 90 A of current is shown by Figure 4.14: 72.58 HV, 80.54 HV, and HV 83.8.

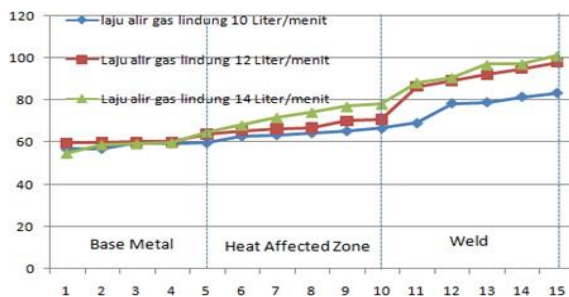


Figure 4.12. Vickers hardness testing graph on 70 A

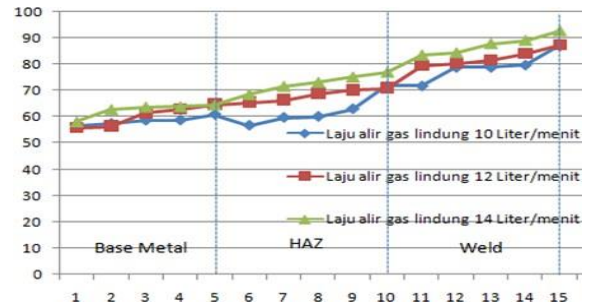


Figure 4.13. Vickers hardness testing graph on 80 A

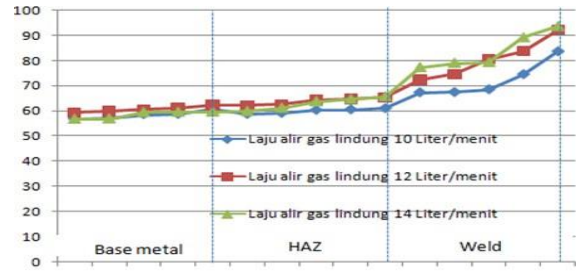


Figure 4.14. Vickers hardness testing graph on 90 A

## 5. CONCLUSION

- 1) The thickness of the intermetallic layer was increased from 70 A to 80 A of current variations, then fell on 90 A of current. The greater the shielding gas flow rate, the thickness of the intermetallic layer will fall.
- 2) The increasing electric current, the hardness will be decreased. Increasingly the protective gas flow rate will increase damage. The highest hardness variations occurred in 70 A of current and 14 L/ min of shielding gas flow rate with 100.9 HV of hardness.

## 6. SUGGESTION

Authors recommend for the next researcher to conduct research on the analysis of the influence of the type of shielding gas and filler metal variations of the mechanical properties of TIG welded joints and steel aluminium.

## REFERENCE

- [1] H. Dong and H. Wenjin, "Detachment of Interfacial Layers During Arc-Brazing of Aluminium Alloy to Carbon Steel with Filler Wire," 2012.
- [2] G. Sierra, P. Peyre, F. Deschaux-Beaume, D. Stuart, and G. Frasn, "Steel to aluminum key-hole laser welding," *Mater. Sci. Eng. A*, no. 447, pp. 197–208, 2007.
- [3] E. Schubert, M. Klassen, I. Zerner, C. Walz, and G. L. Sepold, "Weight structures produced by laser beam joining for future applications in automobile and aerospace industry," *J. Mater. Process. Technol* 2001, no. 115, pp. 2–8, 2001.

- [4] K. Sindou, "Welding Metallurgy Second Edition," 2003.
- [5] S. B. Lin and J. L. Song, "Dissimilar Metal TIG Welding-Brazing of Aluminium Alloy to Galvanized Steel," 2009.
- [6] A. Mathieu and S. Rajasekar, "Dissimilar Material Joining Using Laser (Aluminium to Steel Using Zinc-Based Filler Wire)," 2005.
- [7] H. Fatih, "The Effect of Welding Current on Heat Input, Nugget Geometry, and the Mechanical and Fractural Properties of Resistance Spot Welding on Mg/Al Dissimilar Materials," 2010.
- [8] D. Honggang and H. Wenjin, "Dissimilar Metal Joining Of Aluminium Alloy to Galvanized Steel with Al-Si, Si-Cu, Al-Si-Cu and Zn-Al Filler Wire," 2011.
- [9] L. shao and Y. Shi, "Effect of joining parameters of dissimilar metal joints between aluminium and galvanized steel," 2014.
- [10] Q. Rangfeng and S. Hongxin, "Interfacial of Joint Between Mild Steel and Aluminium Alloy Welded by Resistance Spot Welding," 2010.
- [11] S. Gurjinder and K. Sunil, "Influence Of Current On Microstructure and Hardness of Butt Welding Aluminium AA 6082 Using GTAW Process," 2013.
- [12] G. Qiang and W. Kehong, "Formation and Distribution Mechanism of Intermetallic Compounds Of Al/Mg Joint with Zn Transitional Metal," 2010.